International Journal of Biological Macromolecules 85 (2016) 615–624

Contents lists available at ScienceDirect

International Journal of Biological Macromolecules

journal homepage: www.elsevier.com/locate/ijbiomac

Optimization of carboxymethyl chitosan synthesis using response surface methodology and desirability function

Andrea L. Bukzem[a,*], Roberta Signini[a], Danilo M. dos Santos[a], Luciano M. Lião[b], Diego Palmiro R. Ascheri[a]

[a] Campus de Anápolis de Ciências Exatas e Tecnológicas Henrique Santillo, Universidade Estadual de Goiás (UEG), Br 153 no 3.105—Fazenda Barreiro do Meio, P.O. Box 459, Anápolis, GO 75132-903, Brazil
[b] Instituto de Química, Universidade Federal de Goiás, Campus Samambaia, P.O. Box 131, Goiânia, GO 74001-970, Brazil

ARTICLE INFO

Article history:
Received 1 September 2015
Received in revised form 4 January 2016
Accepted 4 January 2016
Available online 8 January 2016

Keywords:
Carboxymethylation of chitosan
Response surface methodology
Desirability function

ABSTRACT

In this paper, chitosan was reacted with monochloroacetic acid under alkaline conditions to prepare carboxymethyl chitosan. A 2^3 full-factorial central composite design was applied to evaluate the effect of molar ratio sodium hydroxide (NaOH)/Chitosan (Ch), time and molar ratio monochloroacetic acid (MCA)/Chitosan (Ch) on the reaction yield and on the characteristics of carboxymethyl chitosan such as average degree of substitution ($\overline{DS}$) and solubility. An optimization strategy based on response surface methodology was used together with the desirability function approach to optimize this process. The occurrence of carboxymethylation was evidenced by FTIR and ^{1}H NMR spectroscopy. The optimum conditions for carboxymethylation process were found to be 12.4, 10.6 h and 5 for molar ratio sodium hydroxide (NaOH)/Chitosan (Ch), time and molar ratio monochloroacetic acid (MCA)/Chitosan (Ch), respectively. Under these optimal conditions, it was possible to obtain carboxymethyl chitosan with $\overline{DS}$ of 1.86 and solubility of 99.6%. X-ray diffraction and thermogravimetry analysis showed that crystallinity and thermal stability of derivatives was lower than chitosan and decreased with increase of $\overline{DS}$.

1. Introduction

Chitosan is a linear copolymer of β-(1 → 4)-2-amino-2-deoxy-D-glucan (glucosamine-GlcN) and β-(1 → 4)-2-acetamido-2-deoxy-D-glucan (acetylglucosamine-GlcNAc) that is found in cell wall of fungi or may be obtained synthetically by the deacetylation of chitin, an abundant polysaccharide mainly extracted from crustacean cuticles [1,2]. Because of its nontoxicity, biodegradability, and biocompatibility [3,4], a range of applications have been reported for chitosan, including tissue engineering [5], drug delivery [6] and wound dressing [7].

Although chitosan is soluble in aqueous dilute acids below pH 6.5, it is insoluble in neutral water and in common organic solvents [2]. This greatly limits its applications. In this view, several strategies have been adopted for chemical modification of chitosan to improve its water solubility and to expand its range of applications [8,9]. Water-soluble chitosan derivatives can be synthesized by means of carboxymethylation reaction to obtain a derivative known as carboxymethyl chitosan (CMCs) [10].

Carboxymethyl chitosan (CMCs) is a ether derivative, soluble in a wide range of pH and its properties, including high viscosity, large hydrodynamic volume, film- and gel-forming capabilities together with other useful properties, such as biocompatibility, biodegradation, biological activity and low toxicity [11], have been explored in some applications, such as cosmetics [12], foods [13] and pharmaceuticals [14].

Chitosans have three reactive groups in the molecule, that is, a primary hydroxyl group, a secondary hydroxyl group and an amino group [2]. Different reaction conditions allow the preparation of *N*-carboxymethyl chitosan (*N*-CMCs), *O*-carboxymethyl chitosan (O-CMCs) or *N*,*O*-carboxymethyl chitosan (*N*,*O*-CMCs) [15]. *O*-substitution is favored when the carboxymethylation is carried out by reacting chitosan with monochloroacetic acid in isopropanol/aqueous sodium hydroxide under lower temperature, while *N*-substitution predominates in higher temperature [16].

---

* Corresponding author. Fax: +55 62 3328 1177.
E-mail addresses: andrea_bukzem@hotmail.com (A.L. Bukzem), roberta.signini@ueg.br (R. Signini), danilomartins_1@hotmail.com (D.M. dos Santos), luciano@quimica.ufg.br (L.M. Lião), ascheridpr@gmail.com (D.P.R. Ascheri).

http://dx.doi.org/10.1016/j.ijbiomac.2016.01.017
0141-8130/

The synthesis of carboxymethyl chitosan involves reactional parameters such as molar ratio sodium hydroxide (NaOH)/Chitosan (Ch), reaction time and molar ratio monochloroacetic acid (MCA)/Chitosan (Ch) that influence a series of responses related to the important properties of this chitosan derivative as its average degree of substitution ($\overline{DS}$) and solubility in water [10,15–17]. Multivariate approaches based on experimental design are able by at least number of runs to simultaneously consider the interaction of variables, evaluate their main effect and determine the combination of levels that produces the optimum of the process. The response surface methodology (RSM) and desirability function are statistical tools useful to design experiment and construct models that allow to evaluate the effects of multiple factors and investigate optimum conditions [18,19]. In this context, the RSM and desirability function can be considered useful tools to evaluate how the independent variables related to the reaction conditions used to synthesize CMCs, as well as the interactions among them, affect the properties of this chitosan derivative and allow simultaneously optimize the levels of the independent variables aiming to produce highly substituted CMCs exhibiting high solubility in water.

In the present study, carboxymethyl chitosan was prepared applying different molar ratio sodium hydroxide (NaOH)/Chitosan, time and molar ratio monochloroacetic acid (MCA)/Chitosan on synthesis. A 2^3 full-factorial central composite design and response surface methodology were used to evaluate the effects of theses parameters on the average degree of substitution ($\overline{DS}$), solubility and reaction yield of carboxymethyl chitosan. The optimum reaction conditions that favor the obtaining of carboxymethyl chitosan exhibiting high $\overline{DS}$ and solubility were defined using desirability function. Chitosan and its derivatives were characterized by FTIR and ^{1}H NMR spectroscopy, thermogravimetric analysis and X-ray diffraction.

2. Material and methods

2. 1 Reagents

Commercial chitosan extracted from shrimp shells was acquired from Galena Chemicals & Pharmaceuticals Ltd (Campinas, SP; Brazil). The degree of deacetylation ($\overline{DD}$) of chitosan was 90.7% as determined by ^{1}H NMR analysis using a method described in detail in Section 2.4. The molecular weight of chitosan was determined by intrinsic viscosity measurements in 0.3 mol L^{-1} acetic acid/0.2 mol L^{-1} sodium acetate buffer (pH 4.5) at 25.00 ± 0.01 °C. The value of molecular weight was calculated using the Mark–Houwink–Sakurada (MHS) equation and was equal to 5.7×10^3 g mol^{-1} [20]. Monochloroacetic acid (MCA), sodium hydroxide, isopropanol and glacial acetic acid were acquired from Sigma–Aldrich (Saint Louis, MO; USA). All the other reagents were of analytical grade and were used without further purification.

2.2. Synthesis of carboxymethyl chitosan (CMCs)

Synthesis of CMC was carried out under heterogeneous conditions in two steps i.e. alkalization and etherification using a double-walled cylindrical glass reactor coupled to a circulating thermostat at 25 ± 1 °C. Initially, purified chitosan (3 g) was dispersed in isopropanol (65 mL) and 40% of NaOH aqueous solution (9.2–12.4 mol NaOH/mol of chitosan) was added drop wise under magnetic stirring at room temperature over a period of 15 min. After alkalization, monochloroacetic acid (MCA) dissolved in isopropanol (1/1)(5.0–6.5 mol MCA/mol of chitosan) was added under continuous stirring and the reaction mixture was stirred at room temperature for desired duration (6.4–10.6 h). After, the solid product was filtered, suspended in methanol and neutralized with glacial acetic acid. Then, the slurry was filtered and the solid obtained was extensively washed with 80% ethanol to remove undesirable by-products and dried at room temperature.

Table 1
Uncoded and coded levels of the independent variables of the carboxymethylation process.

Independent variables	Symbol	Levels		
		1	0	1
NaOH/Ch (mol/mol)	X_1	9.2	10.8	12.4
Time	X_2	6.4	8.5	10.6
MCA/Ch (mol/mol)	X_3	5.0	5.75	6.5

For the purification of carboxymethyl chitosans, 1.5 g of the sample was dissolved in 750 mL of distilled water. The resulting solution was submitted to positive filtration through 0.45 μm membranes (Millipore®) and added to 18 g NaCl. Then, the carboxymethyl chitosan was precipitated upon addition of absolute ethanol, thoroughly washed with ethanol/water mixtures of increasing ethanol content (70%, 80%, 90%), with absolute ethanol and dried at room temperature. The reaction yield was calculated based on the weights of the parent chitosan and the resulting product.

2.3. Experimental design

A 2^3 full-factorial central composite design was used to analyze the main effects and interactions of the variables molar ratio sodium hydroxide (NaOH)/Chitosan (Ch), time and molar ratio monochloroacetic acid (MCA)/Chitosan (Ch) on the response variables average degree of substitution ($\overline{DS}$), solubility and reaction yield. The independent variables and their levels are shown in Table 1. Maximum and minimum treatment levels were chosen by carrying out preliminary screening tests. A total number of 12 runs of experiment including eight 2^3 orthogonal factorial and four replicate at the center point were carried out.

2.4. ^{1}H NMR spectroscopy

The ^{1}H NMR spectra of chitosan and carboxymethyl chitosan were acquired at 80 °C using a Bruker AVANCE III 500, 11.75 Tesla, spectrometer operating at 500.13 MHz for ^{1}H. CS and CMCs were dissolved in HCl/D$_2$O 1% (v/v) to get the ^{1}H NMR spectra. To get the chitosan and carboxymethyl chitosan spectra, a composite pulse presaturation (CPPR) sequence for water signal suppression was used. The interval between pulses was 3 s, 32 scans were accumulated and the relaxation time was 7 seconds. The spectral window used was 10.0 ppm and the FID size was 32 K. The average degree of deacetylation ($\overline{DD}$), substitution of carboxymethyl groups on 6-O— (f_6), 3-O— (f_3) and 2-N— (f_2) and the total fraction of carboxymethylation (average degree of substitution ($\overline{DS}$) were calculated by treating the ^{1}H NMR spectra according to Eq. (1) [21], Eqs. (2)–(5) [22], respectively.

$$\overline{DD}(\%) = \left(1 - \frac{I_{CH3}/3}{I_{H2-H6}/6}\right) \times 100 \tag{1}$$

$$f_6 = \left(\frac{1}{2}\right)\left(\frac{I_a - I_b}{I_{H2}}\right) \tag{2}$$

$$f_3 = \left(\frac{I_c}{I_{H2}}\right) \tag{3}$$

$$f_2 = \left(\frac{1}{2}\right)\left(\frac{I_c}{I_{H2}}\right) \tag{4}$$

$$\overline{DS} = f_6 + f_3 + f_2 \tag{5}$$

where, I_{CH3} is the integral of the signal due to the methyl hydrogens of GlcNAc units (≈2.0 ppm), I_{H2-H6} is the integral corresponding to the hydrogens H3–H6 from GlcN unit and the hydrogen bonded to C2 of GlcNAc unit (≈3.3–4.0 ppm), I_a is the integral corresponding to the signals of the two protons of carboxymethyl group bonded to C (6) and a hydrogen carboxymethyl group bonded to C (3) (≈4.1–4.3 ppm); I_b is the integral of hydrogen corresponding to a carboxymethyl group bonded to C (3) (≈3.9–4.1 ppm); I_c is the integral corresponding to the two hydrogens from carboxymethyl group bonded to nitrogen group (≈3.2–3.5 ppm); I_{H2} is the integral corresponding to the hydrogen bonded to C(2) of GlcN units (3.15 ppm).

2.5. Fourier transform infrared (FTIR) spectroscopy

Infrared spectra were recorded by using a PerkinElmer FTIR spectrophotometer. Samples were finely ground and mixed with potassium bromide, KBr. The mixture was then compressed into pellet form. FTIR spectral analysis was carried out within the wave number range of 400–4000 cm^{-1}.

2.6. Thermogravimetric analysis (TGA)

The thermal stability of the samples was determined by TGA measurements carried out using a Shimadzu TGA 50 equipment. The amount of sample used for each measurement was approximately 8 mg. All measurements were carried out under a nitrogen atmosphere with a gas flow of 50 mL min^{-1} by heating the material from room temperature to 700 °C at a heating rate of 10 °C min^{-1}.

2.7. X-ray diffraction

XRD patterns of powdered samples were obtained using a Bruker AXS D8 Advance X-ray diffract meter, 40 kV and 40 mA with Cu Kα radiation at k 1.5406 Å. The relative intensity was recorded in the scattering range (2θ) of 5–40° with steps of 0.1° per second.

2.8. Water solubility

The water solubility of the samples was estimated as follows. The weighed sample (100 mg) was suspended in 100 mL distilled water and maintained under magnetic stirring at room temperature for 24 h. Then, the resulting solution was filtered in a positive pressure filter and the precipitates were dried and weighted. The solubility of the sample in water was determined by the percentage of dissolved sample.

2.9. Statistical analysis

The least square multiple regression methodology was used to investigate the relationship between the independent and dependent variables. The multiple regression equation was used to fit the second-order polynomial equation based on the experimental data as follows:

$$Y = \beta_0 + \beta_1 X_1 + \beta_2 X_2 + \beta_3 X_3 + \beta_{12} X_1 X_2 + \beta_{13} X_1 X_3 + \beta_{23} X_2 X_3 + \beta_{123} X_1 X_2 X_3 + \varepsilon \quad (6)$$

where Y represents the predicted response, $^{\beta}{}_0$, is the model intercept, β_1, β_2, β_3, and β_{12}, β_{13}, β_{23}, β_{123}, are linear and interaction coefficients respectively, and X_1, X_2 and X_3 are the independent variables, and ε corresponds to the model residue.

The statistical significance of the each individual coefficient term was determined by evaluating the p-value and F-value with 95% confidence level obtained from the analysis of variance (ANOVA). The lack of fit of regression model was evaluated with 95% confidence level. The extent of fitting of the experimental results to the polynomial model equation was expressed by the coefficient of determination (R^2) and adjusted coefficient of determination ($R^2{}_{adj}$). Response surfaces of the present design were achieved by using the fitted model and keeping one independent variable constant while varying the other two variables. Once an adjusted response to the polynomial model was obtained, the best conditions of carboxymethylation were defined using desirability function [18]. All calculations and graphics were performed with Statistica software (Statsoft version 7.0, USA).

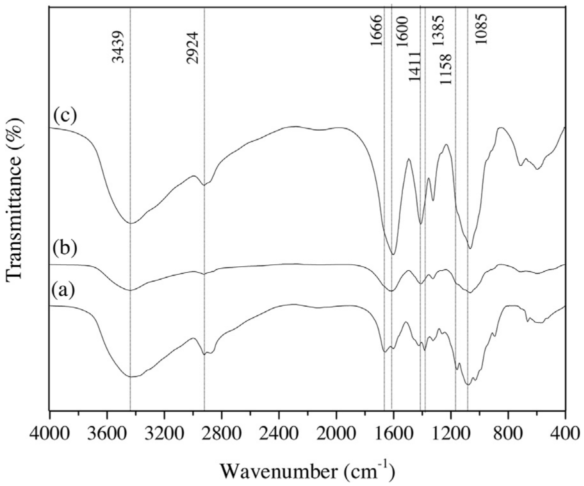

Fig. 1. FTIR spectrum of chitosan (a) and samples T4 (b) and T8 (c).

3. Results and discussion

The synthesis of carboxymethyl chitosan involved two reaction steps. In the first step, chitosan was treated with NaOH, in the presence of isopropanol, which acted both as a swelling agent and as a dilutant facilitateing the penetration of NaOH into the chitosan structure. The second step consisted in reaction of alkali chitosan and monochloroacetic acid [12]. The occurrence of carboxymethylation and the presence of characteristic functional groups of chitosan (CS) and carboxymethyl chitosan (CMCs) were confirmed by infrared and^{1}H NMR spectroscopy.

3.1. Fourier transform infrared (FTIR) spectroscopy

FTIR spectra of CS (Fig. 1(a)) shows basic characteristic absorption bands at 3440 cm^{-1} (O—H and N—H stretch), 1666 cm^{-1} (stretching of C═O amide group), 1598 cm^{-1} (angular deformation of the N—H bonds of the amino groups), 1385 cm^{-1} (symmetric angular deformation of CH_3), 1158 cm^{-1} (asymmetric bridge-O-stretch) and 1085 cm^{-1} (skeletal vibration involving the C—O stretch) [23]. The FTIR spectrum of CMCs (Fig. 1(b) and(c)) shows the occurrence of an intense band at 1600 cm^{-1} and a moderate band at 1411 cm^{-1} due to the symmetric and asymmetric axial deformations of COO^-, respectively, which confirms the introduction of the carboxymethyl groups [16,24].

3.2. ^{1}H NMR data analysis

Additional evidence for the structure of the modified chitosan is provided by comparison of the ^{1}H NMR spectra obtained for chitosan (Fig. 2a) and carboxymethyl chitosan (Fig. 2b). The ^{1}H NMR spectrum of chitosan exhibited a singlet at 2.0 ppm characteristic of methyl hydrogens of GlcNAc units, a signal at 3.18 ppm related to the hydrogen bonded to C(2) of GlcN units, the set of signals in the range of 3.4–4.0 ppm corresponding to the hydrogens H(3)–H(6) from GlcN unit and the hydrogen bonded to C(2)

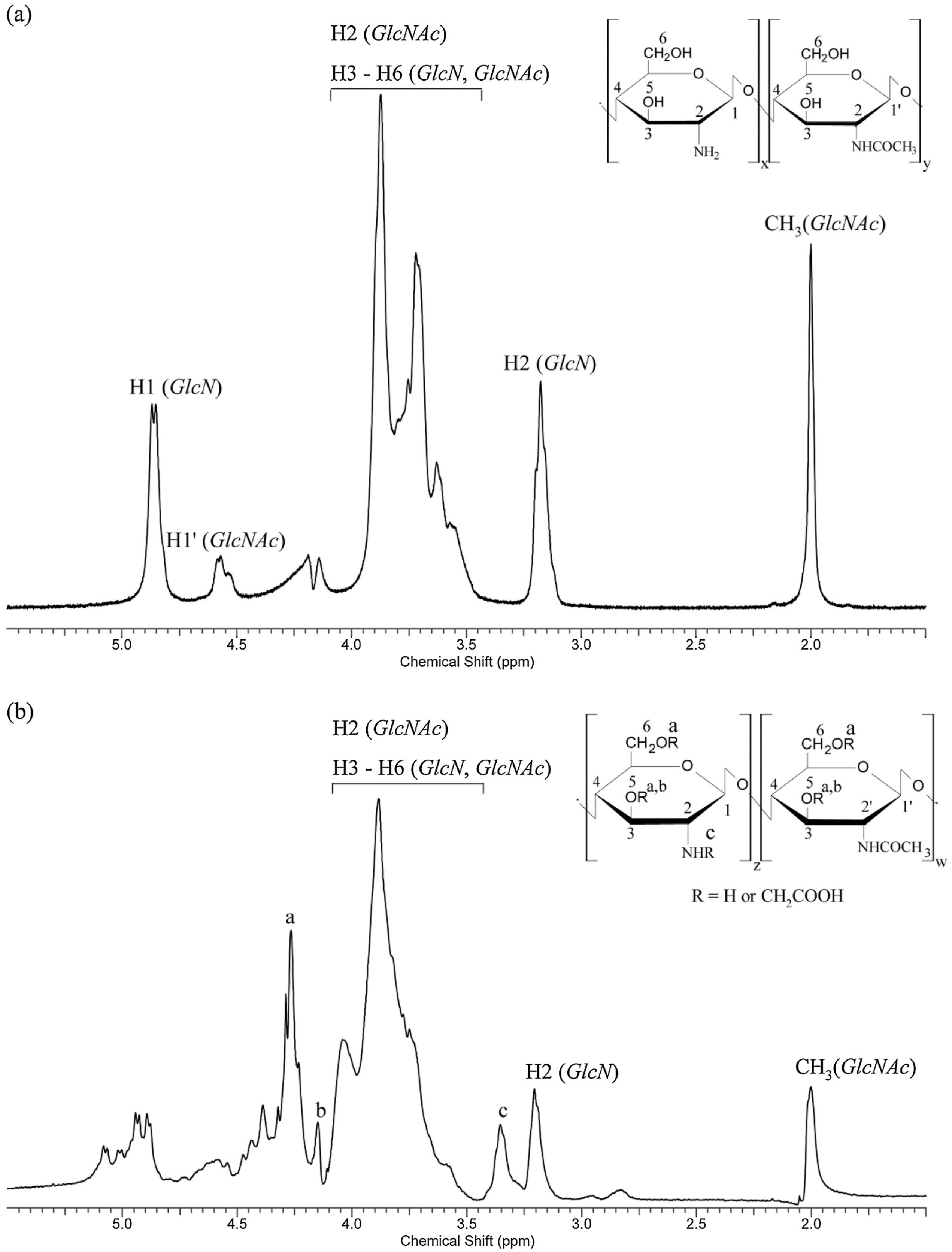

Fig. 2. ^{1}H NMR spectra of chitosan (a) and sample T7 (b) in solution D_2O/HCl 1% (v/v) acquired at 80 °C.

Table 2
-Independent variables of the 2^3 full-factorial central composite design and the experimental results.

Runs	Factors[a]			Responses[b]					
	X_1	X_2	X_3	$\overline{DS}$	% f_6	% f_3	% f_2	Sol. (%)	Yield (%)
1	9.2 (−1)	6.4 (−1)	5.0 (−1)	0.84	69.5	8.7	21.8	85.5	84.7
2	9.2 (−1)	6.4 (−1)	6.5 (+1)	1.73	58.3	19.6	22.1	99.4	146.5
3	9.2 (−1)	10.6 (+1)	5.0 (-1)	1.38	59.3	18.0	22.7	97.8	130.3
4	9.2 (−1)	10.6 (+1)	6.5 (+1)	0.45	40.9	26.8	32.3	55.4	41.2
5	12.4 (+1)	6.4 (−1)	5.0 (−1)	0.82	72.1	6.6	21.3	75.5	159.1
6	12.4 (+1)	6.4 (−1)	6.5 (+1)	1.46	36.0	36.4	27.65	98.6	149.5
7	12.4 (+1)	10.6 (+1)	5.0 (−1)	1.86	59.9	16.3	23.8	99.6	140.9
8	12.4 (+1)	10.6 (+1)	6.5 (+1)	1.61	57.5	21.5	21.0	99.3	121.9
9	10.8 (0)	8.5 (0)	5.75 (0)	1.34	60.4	24.1	15.5	93.9	129.4
10	10.8 (0)	8.5 (0)	5.75 (0)	1.28	58.0	23.9	18.1	91.3	133.9
11	10.8 (0)	8.5 (0)	5.75 (0)	1.13	60.7	22.1	17.2	87.2	133.3

[a] X_1 = molar ratio sodium hydroxide (NaOH)/Chitosan (Ch); X_2 = time (h); X_3 = molar ratio monochloroacetic acid (MCA)/Chitosan (Ch).

[b] Average degree of substitution; f_6; f_3 and f_2 are the fractions of carboxymethylation at the position 6-O—, 3-O— and 2-N—; Sol.: solubility in water.

of GlcNAc unit, while those signals occurring at 4.57 ppm and 4.86 ppm are attributed to the hydrogen bonded to the anomeric carbon (C(1)) of GlcNAc(H(1)′) and GlcN(H(1)) units, respectively [22,25,26]. From this spectral analysis and taking into account Eq. (2), the average degree of deacetylation was determined as 90.7%.

The ^{1}H NMR spectrumof the carboxymethyl chitosan show signals between 4.20–4.34 ppm corresponding to signals of the two hydrogens of carboxymethyl group bonded to C(6) and a hydrogen carboxymethyl group bonded to C(3) (a) [22]. The set of signals in the range of 4.12–4.19 ppm are attributed to hydrogen ofcarboxymethyl group bonded to C(3)(b). In addition, the occurrence of *N*-carboxymethylation was evidenced by the signals in the range of 3.25–3.45 ppm assigned to the two hydrogens from carboxymethyl group bonded to nitrogen group (c) [22,27]. The substitution of carboxymethyl groups on 6-O— (f_6), 3-O— (f_3) and 2-N— (f_2) and the average degree of substitution ($\overline{DS}$) were calculated from the corresponding ^{1}H NMR spectra by using Eqs. (2)–(5), respectively. The results obtained with the experimental design for carboxymethyl groups arrangement,$\overline{DS}$, solubility and yield after purification are shown in Table 2.

3.3. Statistical analysis and model fitting

In the carboxymethyl chitosan synthesis the three possible positions on the chitosan group are on the C(3), C(6) and NH_2 bonded to C(2) from the chitosan polymeric chain. It can be observed from Table 2 that the carboxymethylationon position 6 is higher than on positions 2 and 3, with exception of run 6, and that *O*-carboxymethylation predominated in all samples. Additionally, the average degree of substitution ranged between 0.45 and 1.86.

The solubility of CMCs ranged between 55.4 and 99.6% showing a strong positive linear correlation ($R^2 = 0.92$) with the average degree of substitution, i.e. highest solubility was observed for samples with highest $\overline{DS}$. Similar findings were reported by Chen and Park [15] and Bidgoli et al. [28]. Moreover, it can be seen on Table 2 that the reaction yields were between 41.2 and 159.1% and do not present linear correlation with $\overline{DS}$. These results show that the reaction conditions strongly affect the characteristics of the resulting CMCs and the reaction yield.

In order to describe the relationship between the dependent variables and the independent variables, Eq. (6) was fitted to the experimental data by multiple regression analysis and the fit of the model was evaluated by means of ANOVA tests which showed the terms of the model that were statistically significant for a confidence level of 95% (p-value <0.05), and those that were not statistically significant. The results of ANOVA for all responses are listed in Table 3.

The lack of fit is an indication of the failure for a model representing the experimental data in which points are not included in the regression or variations in the models cannot be accounted for random error. With the exception of the variable response yield, no lack of fit of the models was observed at a significance level of 5% (p-value >0.05). The F-test and p-value were used to measure the significance of the coefficients of the model and the corresponding terms are more significant if the absolute F-value becomes greater and the p-value becomes smaller. It can be seen from Table 3 that the predominant effect on the developed model for the degree of substitution corresponded to the interaction term between time and molar ratio monochloroacetic acid (MCA)/Chitosan (Ch)($X_2.X_3$), followed by the interaction term between molar ratio sodium hydroxide (NaOH)/Chitosan (Ch) and time ($X_1.X_2$) and the linear term molar ratio NaOH/Ch(X_1).

The solubility was severely influenced by the interaction term between time and molar ratio MCA/Ch ($X_2.X_3$), followed by the interaction term between molar ratio NaOH and time ($X_1.X_2$) and interaction term between molar ratio NaOH/Ch and molar ratio MCA/Ch ($X_2.X_3$), as can be observed in Table 3.

The fitted models for $\overline{DS}$ and solubility both without insignificant terms and in uncoded form are given in Eqs. (7) and (8), respectively.

$$\overline{\text{DS}} = 1.49\text{X}_1 + 3.35\text{X}_2 + 5.64\text{X}_3 - 0.19\text{X}_1\text{X}_2 - 0.35\text{X}_1\text{X}_3 - 0.71\text{X}_2\text{X}_3 + 0.05\text{X}_1\text{X}_2\text{X}_3 - 25.93 \tag{7}$$

Table 3
Analysis of variance (ANOVA) results.

Term	Responses					
	$\overline{DS}$		Solubility		Yield	
	F-value	p-Value	F-Value	p-Value	F-Value	p-Value
X_1	19.47**	0.047	13.30 ns	0.067	572.46*	0.001
X_2	2.16 ns	0.279	0.50 ns	0.550	224.24*	0.004
X_3	1.30 ns	0.371	0.34 ns	0.618	62.82**	0.015
$X_1.X_2$	39.79**	0.024	34.77**	0.028	3.93 ns	0.185
$X_1.X_3$	1.97 ns	0.295	28.77**	0.033	0.04 ns	0.866
$X_2.X_3$	78.46**	0.012	69.54**	0.014	517.26*	0.001
$X_1.X_2.X_3$	9.24 ns	0.093	11.78 ns	0.075	402.64*	0.002
Lack of fit	0.066 ns	0.821	0.672 ns	0.498	38.53**	0.024982
$R^2_{\text{aj.}}$	0.9554		0.9449		0.9259	

[a] X_1 = molar ratio sodium hydroxide (NaOH)/Chitosan (Ch) (mol mol^{-1}); X_2 = time (h); X_3 = molar ratio monochloroacetic acid (MCA)/Chitosan (Ch) (mol mol^{-1}); ns = non significant.

[*] Significant at 1% probability ($p < 0.01$).

[**] Significant at 5% probability ($p < 0.05$).

$$\begin{aligned}\text{Solubility}(\%) &= 33.8X_1 + 114.5X_2 + 144.7X_3 - 7.3X_1X_2 \\ &\quad - 8.5X_1X_3 - 23.9X_2X_3 + 1.63X_1X_2X_3\ 575.9 \end{aligned} \tag{8}$$

The models for degree of substitution and solubility showed a good fit with the experimental data, as the value of adjusted determination coefficient ($R^2{}_{\text{adj.}}$) were 0.9554 and 0.9449, respectively. This confirms that the fitted models could explain more than 94.00% of the total variability within the range of values studied.

Three-dimensional surfaces were generated based on Eqs. (7) and (8) and are shown in Fig. 3 which presents the relationship between the variables of the three processes in each response. The effects of molar ratio (NaOH)/Ch(X_1) and time (X_2) and molar ratio MCA/Ch(X_3) on the $\overline{DS}$ are shown in Fig. 3A–C. We found that an increase in the reaction time and the molar ratio of sodium hydroxide results in larger values of$\overline{DS}$. The enhancement of $\overline{DS}$ with the increase of molar ratio of sodium hydroxide solution and duration of reaction may be due to the fact that a better reaction environment is created (best alkalization of chitosan resulting in a higher number of hydroxyl groups deprotonated and hence better efficiency in the subsequent step etherification) and a prolonged time allows more complete reactions.

Fig. 3B shows that the $\overline{DS}$ increases when larger amounts of hydroxide and acid are used. This may be due to the greater availability of the acid molecules at higher concentrations in the proximity of the chitosan with the highest number of hydroxyl groups deprotonated. However, it may observed in Fig. 3B that with a lower molar ratio of NaOH and high molar ratio of acid, the value of $\overline{DS}$ decreases. This can be attributed to the lower number of hydroxyl groups deprotonated when lower amounts of NaOH are employed.

The response surface plot to $\overline{DS}$ as a function of the reaction time and the quantity of acid that keeps the molar ratio NaOH fixed at the center point value (Fig. 3C) shows that the increase in reaction time in conjunction with the use of smaller molar ratio of acid results in higher values of $\overline{DS}$.

The response surface plots to solubility (Fig. 3D–F) clearly shows that high reaction time combined with a smaller molar ratio of acid and high molar ratio of NaOH increased the value of solubility. The surfaces obtained for solubility exhibit a behavior similar to that shown by the degree of substitution with respect to the independent variables under study, indicating that the chitosan derivatives are more soluble in water with a higher $\overline{DS}$. These results are in agreement with the work of Mourya et al. [17].

3.4. Optimization of the carboxymethylation process

The desirability function [18] was employed to simultaneously optimize the levels of the independent variables aiming to produce highly substituted CMCs exhibiting high solubility in water. Thus, an individual desirability function, *d*, is proposed for a given response, *y*, whose values are expressed by using a non-dimensional scale ranging in the interval 0–1 and aiming the response maximization, its corresponding individual desirability function is of the type the-larger-the-best, the conversion scheme being given by:

$$d = \left\{ \begin{array}{ll} 0 & \text{if}\, y \le y^{\min} \\ \left(\dfrac{y - y^{\min}}{y^{\max} - y^{\min}}\right)^{w} & \text{if}\, y^{\min} \le y \le y^{\max} \\ 1 & \text{if }\ y \ge y^{\max} \end{array} \right. \tag{9}$$

where *y* is the response value, $y_{\min}$ and $y_{\max}$ are the lower- and upper-bound limit of the response, respectively, and *w* is the weight coefficient (in this case $w = 1$). The global desirability is determined by taking into account all individual desirability functions by:

$$D = \left(\prod_{h=1}^{m} d_h\right)^{1/m} \tag{10}$$

Table 4
Characteristic temperatures for the two first stages of the thermal degradation of the chitosan and carboxymethylated samples from the corresponding TG and DTG curves.

Sample	Stage I			Stage II		
	Range	$T_{\text{MÁX}}$ (°C)	WL (%)	Range	$T_{\text{onset}}{}^{*}$ (°C)	WL** (%)
Chitosan	25–150	63	9	220–420	280	43
T4	25–150	64	14	180–400	268	40
T7	25–150	64	16	200–360	262	31

The optimization algorithm allowed the elaboration of the profiles for predicted response values and desirability functions (Fig. 4), the vertical red lines shown in the upper three rows of curves indicating the maximal individual desirability relative to average degree of substitution and solubility while the bottom row show the maximum global desirability. This analysis show that the maximum global desirability, $D = 0.9982$, is reached when the optimized reaction conditions are employed, i.e. high molar ratio sodium hydroxide (NaOH)/chitosan (Ch) (12.4), long reaction time (10.6 h) and low molar ratio monochloroacetic acid (MCA)/Chitosan (Ch) (5). Thus, the use of such experimental conditions when carrying out the extensive carboxymethylation of chitosan will result in sample exhibiting high average degree of substitution (1.86) and solubility (99.61%).

3.5. Thermogravimetric analysis

Chitosan and carboxymethyl chitosan achieved from run 4 (T4) and run 7 (T7) were also characterized by thermogravimetry (TG) and X-ray diffraction (XRD). Fig. 5a and b shows the TG and derivative thermogravimetry DTG curves, respectively, obtained for chitosan and samples T4 and T8. The corresponding data of the main thermal events are listed in Table 4. In all cases, the first thermal event occurs due to the evaporation of adsorbed and bound water in the temperature range 25–150 °C, where all samples present a mass loss ranging from 9% to 14%.

According to the results presented in Table 4, chitosan derivatives exhibit greater weight loss at this stage because carboxymethylation enhances their hydrophilicity. Moreover, the derivative with the higher average degree of substitution (T7) presents higher loss of mass in this temperature interval than the less substituted derivative (T4).

The second thermal event starts at about 220 °C and extends to 420 °C for chitosan and occurs in the temperature range 180–400 °C and 200–360 °C for samples T4 and T7, respectively, and is accompanied with weight loss of 43%, 40% and 31% for chitosan, T4 and T7, respectively (Table 4). In addition, the onset temperature for chitosan, T4 and T7 were 280 °C, 268 °C and 262 °C, respectively. This thermal event corresponds to the decomposition of chitosan's main chain and cleavage of substituent groups in the carboxymethylated derivatives. The complete thermal decomposition of the polymers occurs at temperatures higher than 420 °C, 400 °C and 360 °C for chitosan, T4 and T7 samples, respectively. As may be observed, the thermal stability of carboxymethylated samples reduced with the increase in the degree of substitution and was lower than that of chitosan. Similar findings were reported for other chitosan derivatives [29–31].

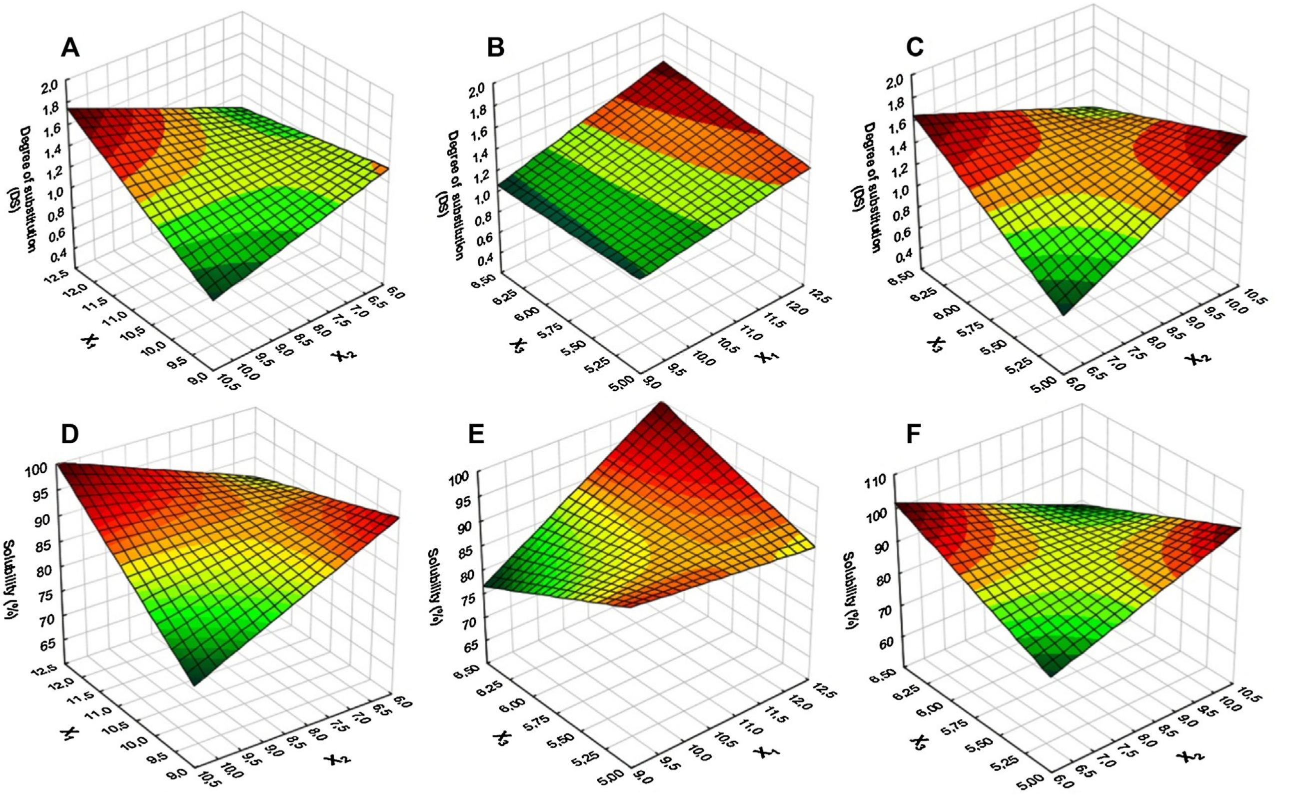

Fig. 3. Response surface plots show the effect of mass of molar ratio sodium hydroxide (NaOH)/Chitosan (Ch) (X_1); time (X_2) and molar ratio monochloroacetic acid (MCA)/Chitosan (Ch) (X_3) on the response variables degree of substitution (A–C) and solubility (D–F).

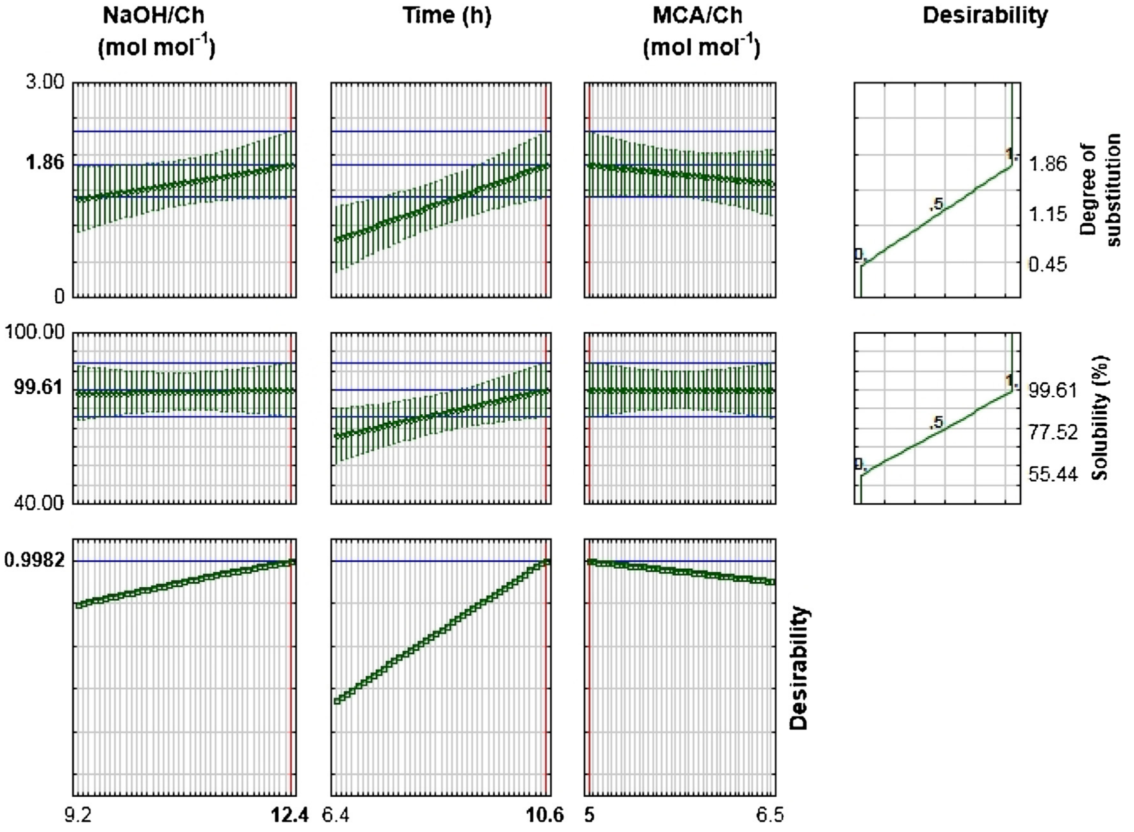

Fig. 4. Profiles of predicated response values and desirability function. Red line indicated current values after optimization. (For interpretation of the references to color in this figure legend, the reader is referred to the web version of this article.)

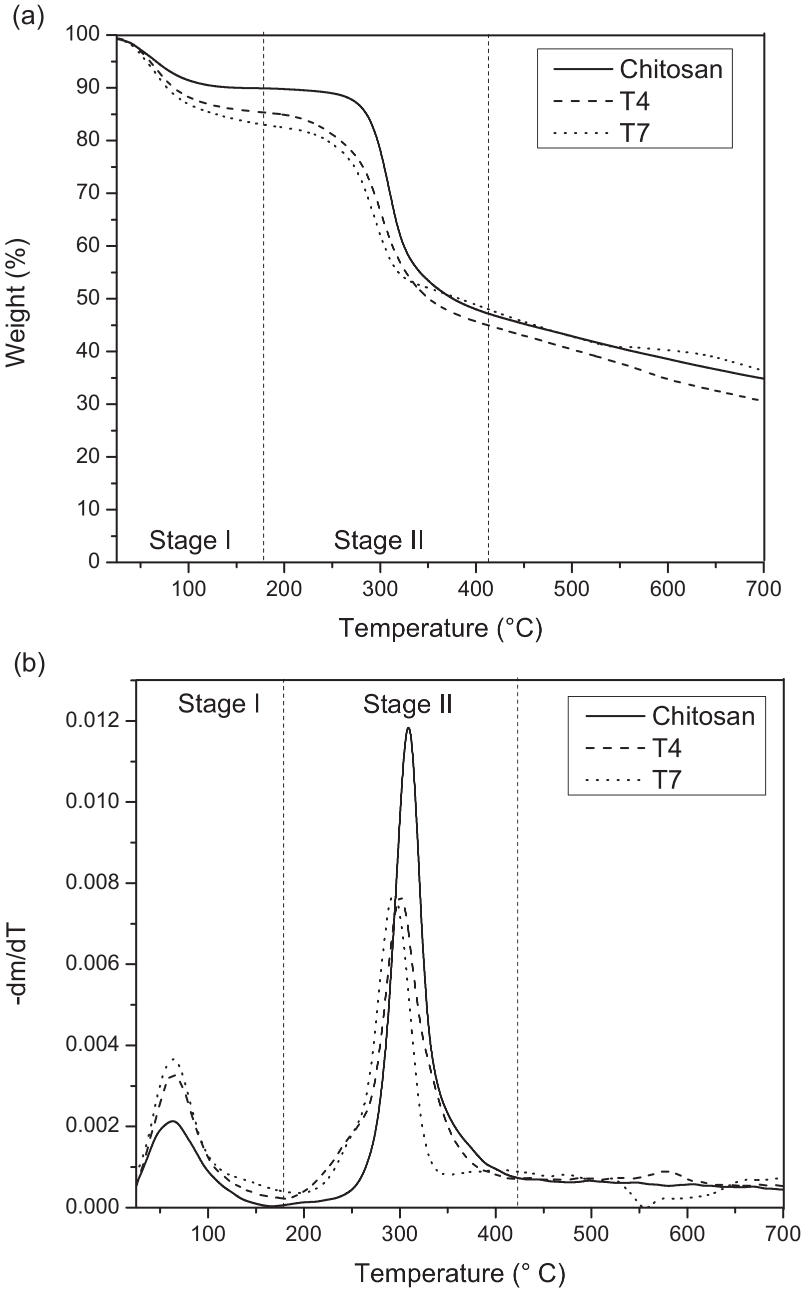

Fig. 5. (a) TG and (b) DTG of chitosan and samples T4 and T7.

3.6. X-ray diffraction

The XRD analysis was conducted to compare the crystanillinity of chitosan and carboxymethylated derivative as presented in Fig. 6. It is observed that the diffractogram of unmodified chitosan has a main peak at $2\theta = 20.0^\circ$ related to the reflection of (2 0 0) plane and other at $2\theta = 10.4^\circ$ corresponding to the (0 2 0) plane [32]. For the chitosan derivatives, the peak at 10.4° and the peak at 20.0° significantly decreased with increasing the $\overline{DQ}$. The crystallinity index (CrI) of all samples was calculated following the method proposed by Osorio-Madrazo et al. [32]. By this method, the CrI was found to be 38.0, 24.5 and 20.2% for chitosan, T4 and T7, respectively. These results suggest that the arrangement of the polymer chains in the solid state has changed upon the derivatization of chitosan and that its degree of order was significantly decreased as a consequence of the introduction of a large number of bulky and charged substituents which disrupte hydrogen bonding and impart an important steric hindrance [33].

4. Conclusions

Carboxymethyl chitosan with different average degrees of substitution and solubility were obtained in accordance with the reaction conditions used. FTIR and ^{1}H NMR analysis of the derivative confirmed the incorporation of the carboxymethyl groups. The most significant variable affecting the average degree of substitution is the interaction term between time and molar ratio monochloroacetic acid/chitosan, followed by the interaction term between molar ratio sodium hydroxide/chitosan and time and the linear terms molar ratio sodium hydroxide/chitosan. The variables

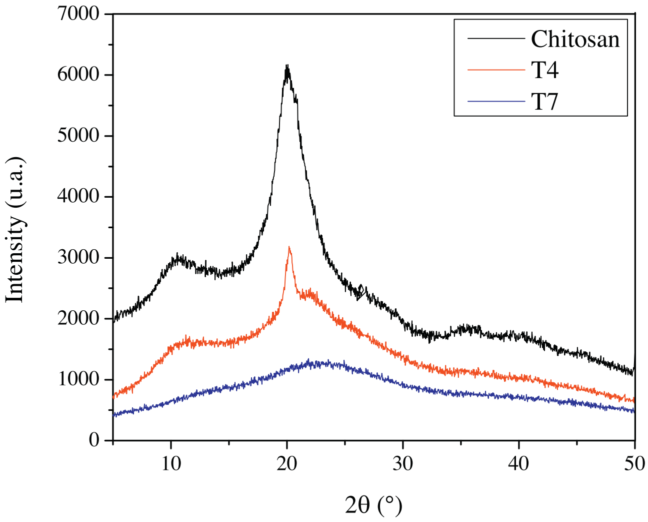

Fig. 6. X-ray diffractograms of chitosan and samples T4 and T7.

with the largest effect on solubility were the interaction term between time and molar ratio monochloroacetic acid/chitosan, followed by the interaction term between molar ratio sodium hydroxide/chitosan and time and interaction term between molar ratio sodium hydroxide/chitosan and molar ratio monochloroaceticacid/chitosan. For the optimization of the carboxymethylation process, the desirability function approach was used. The optimum conditions for carboxymethylation process were found to be 12.4, 10.6 h and 5 for molar ratio sodium hydroxide/Chitosan and time and molar ratio monochloroacetic acid/chitosan, respectively, for which the desirability was $D = 0.9982$. Under this optimum condition, it was possible to obtain carboxymethyl chitosan with an average degree of substitution of 1.86 and solubility of 99.6%. X-ray diffraction and thermogravimetric analyses revealed that the crystallinity and thermal stability of carboxymethylated samples were lower than those of chitosan and decreased with increasing $\overline{DS}$.

Acknowledgements

The authors would like to thank the Universidade Estadual de Goiás (UEG) for the research stimulation grant (PROBIP) and revision of the article. Coordenação de Aperfeiçoamento de Pessoal de Nível Superior (CAPES, Brazil), Conselho Nacional de Desenvolvimento Científico e Tecnológico (CNPq, Brazil) and Fundação de Amparo à Pesquisa do Estado de Goiás (FAPEG) for their financial support.

References

[1] I. Aranaz, M. Mengíbar, R. Harris, I. Paños, B. Miralles, N. Acosta, et al., Functional characterization of chitin and chitosan, Curr. Chem. Biol. 3 (2009) 203–230.
[2] R.A.A. Muzzarelli, C. Muzzarelli, Chitosan Chemistry: Relevance to the Biomedical Sciences, in: T. Heinze (Ed.), Polysaccharides I SE—136820, vol. 186, Springer, Berlin, Heidelberg, 2005, pp. 151–209, http://dx.doi.org/10.1007/b136820.
[3] T.A. Sonia, C. Sharma, Chitosan and Its Derivatives for Drug Delivery Perspective, in: R. Jayakumar, M. Prabaharan, R.A.A. Muzzarelli (Eds.), Chitosan Biomater. I SE—117, vol. 243, Springer, Berlin, Heidelberg, 2011, pp. 23–53, http://dx.doi.org/10.1007/12_2011_117.
[4] S. Kaur, G.S. Dhillon, The versatile biopolymer chitosan: potential sources, evaluation of extraction methods and applications, Crit. Rev. Microbiol. 40 (2014) 155–175.
[5] S.K.L. Levengood, M. Zhang, Chitosan-based scaffolds for bone tissue engineering, J. Mater. Chem. B 2 (2014) 3161–3184.
[6] M.-X. Chen, B.-K. Li, D.-K. Yin, J. Liang, S.-S. Li, D.-Y. Peng, Layer-by-layer assembly of chitosan stabilized multilayered liposomes for paclitaxel delivery, Carbohydr. Polym. 111 (2014) 298–304.
[7] G.D. Mogoşanu, A.M. Grumezescu, Natural and synthetic polymers for wounds and burns dressing, Int. J. Pharm. 463 (2014) 127–136, http://dx.doi.org/10.1016/j.ijpharm.2013.12.015.
[8] E. Faizuloev, A. Marova, A. Nikonova, I. Volkova, M. Gorshkova, V. Izumrudov, Water-soluble *N*-[(2-hydroxy-3-trimethylammonium)propyl]chitosan chloride as a nucleic acids vector for cell transfection, Carbohydr. Polym. 89 (2012) 1088–1094.
[9] T. Chivangkul, S. Pengprecha, P. Padungros, K. Siraleartmukul, S. Prasongsuk, N. Muangsin, Enhanced water-solubility and mucoadhesion of *N*,*N*,*N*-trimethyl-*N*-gluconate-*N*-homocysteine thiolactone chitosan, Carbohydr. Polym. 108 (2014) 224–231.
[10] L. Upadhyaya, J. Singh, V. Agarwal, R.P. Tewari, Biomedical applications of carboxymethyl chitosans, Carbohydr. Polym. 91 (2013) 452–466.
[11] L. Upadhyaya, J. Singh, V. Agarwal, R.P. Tewari, The implications of recent advances in carboxymethyl chitosan based targeted drug delivery and tissue engineering applications, J. Control. Release 186 (2014) 54–87.
[12] A. Jimtaisong, N. Saewan, Utilization of carboxymethyl chitosan in cosmetics, Int. J. Cosmet. Sci. 36 (2014) 12–21, http://dx.doi.org/10.1111/ics.12102.
[13] M. Qiu, C. Wu, G. Ren, X. Liang, X. Wang, J. Huang, Effect of chitosan and its derivatives as antifungal and preservative agents on postharvest green asparagus, Food Chem. 155 (2014) 105–111, http://dx.doi.org/10.1016/j.foodchem.2014.01.026.
[14] J.R. Bresolin, M.-C.T. Largura, C.C. Dalri, G. Hoffer, C.A. Rodrigues, R.M. Lucinda-Silva, Spray-dried *O*-carboxymethyl chitosan as potential hydrophilic matrix tablet for sustained release of drug, Drug Dev. Ind. Pharm. 40 (2014) 503–510.
[15] X.-G. Chen, H.-J. Park, Chemical characteristics of *O*-carboxymethyl chitosans related to the preparation conditions, Carbohydr. Polym. 53 (2003) 355–359, http://dx.doi.org/10.1016/S0144-8617(03)00051-1.
[16] F.R. De Abreu, S.P. Campana-Filho, Characteristics and properties of carboxymethylchitosan, Carbohydr. Polym. 75 (2009) 214–221, http://dx.doi.org/10.1016/j.carbpol.2008.06.009.
[17] V. Mourya, N.N. Inamdar, A. Tiwari, Carboxymethyl chitosan and its applications, Adv. Mater. Lett. 1 (2010) 11–33, http://dx.doi.org/10.5185/amlett.2010.3108.
[18] G. Derringer, R. Suich, Simultaneous-optimization of several response variables, J. Qual. Technol. 12 (1980) 214–219.
[19] R.H. Myers, D.C. Montgomery, C.M. Anderson-Cook, Response Surface Methodology: Process and Product Optimization Using Designed Experiments, 3rd ed., John Wiley & Sons, Ltd., Hoboken, New Jersey, 2009.
[20] M. Rinaudo, M. Milas, P. Le Dung, Characterization of chitosan. Influence of ionic strength and degree of acetylation on chain expansion, Int. J. Biol. Macromol. 15 (1993) 281–285, http://dx.doi.org/10.1016/0141-8130(93)90027-J.
[21] A. Hirai, H. Odani, A. Nakajima, Determination of degree of deacetylation of chitosan by 1H NMR spectroscopy, Polym. Bull. 26 (1991) 87–94, http://dx.doi.org/10.1007/BF00299352.
[22] R.J.N. Hjerde, K.M. Vårum, H. Grasdalen, S. Tokura, O. Smidsrød, Chemical composition of *O*-(carboxymethyl)-chitins in relation to lysozyme degradation rates, Carbohydr. Polym. 34 (1997) 131–139, http://dx.doi.org/10.1016/S0144-8617(97)00113-6.
[23] J. Brugnerotto, J. Lizardi, F.M. Goycoolea, W. Argüelles-Monal, J. Desbrières, M. Rinaudo, An infrared investigation in relation with chitin and chitosan characterization, Polymer (Guildf.) 42 (2001) 3569–3580, http://dx.doi.org/10.1016/S0032-3861(00)00713-8.
[24] Z. Zhao, Z. Wang, N. Ye, S. Wang, A novel *N*,*O*-carboxymethyl amphoteric chitosan/poly(ethersulfone) composite MF membrane and its charged characteristics, Desalination 144 (2002) 35–39, http://dx.doi.org/10.1016/S0011-9164(02)00285-0.
[25] M. Rinaudo, Chitin and chitosan: properties and applications, Prog. Polym. Sci. 31 (2006) 603–632, http://dx.doi.org/10.1016/j.progpolymsci.2006.06.001.
[26] J. Desbrières, C. Martinez, M. Rinaudo, Hydrophobic derivatives of chitosan: characterization and rheological behaviour, Int. J. Biol. Macromol. 19 (1996) 21–28, http://dx.doi.org/10.1016/0141-8130(96)01095-1.
[27] R.A.A. Muzzarelli, P. Ilari, M. Petrarulo, Solubility and structure of *N*-carboxymethylchitosan, Int. J. Biol. Macromol. 16 (1994) 177–180, http://dx.doi.org/10.1016/0141-8130(94)90048-5.
[28] H. Bidgoli, A. Zamani, M.J. Taherzadeh, Effect of carboxymethylation conditions on the water-binding capacity of chitosan-based superabsorbents, Carbohydr. Res. 345 (2010) 2683–2689, http://dx.doi.org/10.1016/j.carres.2010.09.024.
[29] D. De Britto, S.P. Campana-Filho, A kinetic study on the thermal degradation of *N*,*N*,*N*-trimethylchitosan, Polym. Degrad. Stab. 84 (2004) 353–361, http://dx.doi.org/10.1016/j.polymdegradstab.2004.02.005.
[30] T. Xu, M. Xin, M. Li, H. Huang, S. Zhou, Synthesis, characteristic and antibacterial activity of *N*,*N*,*N*-trimethyl chitosan and its carboxymethyl derivatives, Carbohydr. Polym. 81 (2010) 931–936, http://dx.doi.org/10.1016/j.carbpol.2010.04.008.
[31] P.D. Chethan, B. Vishalakshi, L. Sathish, K. Ananda, B. Poojary, Preparation of substituted quaternized arylfuran chitosan derivatives and their antimicrobial activity, Int. J. Biol. Macromol. 59 (2013) 158–164, http://dx.doi.org/10.1016/j.ijbiomac.2013.04.045.

[32] A. Osorio-Madrazo, L. David, S. Trombotto, J.-M. Lucas, C. Peniche-Covas, A. Domard, Kinetics study of the solid-state acid hydrolysis of chitosan: evolution of the crystallinity and macromolecular structure, Biomacromolecules 11 (2010) 1376–1386, http://dx.doi.org/10.1021/bm1001685.

[33] B. Xiao, Y. Wan, X. Wang, Q. Zha, H. Liu, Z. Qiu, et al., Synthesis and characterization of *N*-(2-hydroxy)propyl-3-trimethyl ammonium chitosan chloride for potential application in gene delivery, Colloids Surf. B Biointerfaces 91 (2012) 168–174, http://dx.doi.org/10.1016/j.colsurfb.2011.10.053.